THE JOURNAL OF PHYSICAL CHEMISTRY B

Article

pubs.acs.org/JPCB

How Does the Ionic Liquid Organizational Landscape Change when Nonpolar Cationic Alkyl Groups Are Replaced by Polar Isoelectronic Diethers?

Hemant K. Kashyap,[†] Cherry S. Santos,[‡] Ryan P. Daly,[†] Jeevapani J. Hettige,[†] N. Sanjeeva Murthy,[§] Hideaki Shirota,[∥] Edward W. Castner, Jr.,*[,‡] and Claudio J. Margulis*[,†]

[†]Department of Chemistry, University of Iowa, Iowa City, Iowa 52242, United States

[‡]Department of Chemistry and Chemical Biology, Rutgers, The State University of New Jersey, Piscataway, New Jersey 08854, United States

[§]New Jersey Center for Biomaterials, Rutgers, The State University of New Jersey, Piscataway, New Jersey 08854, United States

[∥]Department of Nanomaterial Science and Department of Chemistry, Chiba University, 1-33 Yayoi, Inage-ku, Chiba 263-8522, Japan

Supporting Information

ABSTRACT: X-ray scattering experiments and molecular dynamics simulations have been performed to investigate the structure of four room temperature ionic liquids (ILs) comprising the bis(trifluoromethylsulfonyl)amide (NTf_2^-) anion paired with the triethyloctylammonium (N_{2228}^+) and triethyloctylphosphonium (P_{2228}^+) cations and their isoelectronic diether analogs, the (2-ethoxyethoxy)ethyltriethylammonium ($N_{222(2O2O2)}^+$) and (2-ethoxyethoxy)ethyltriethylphosphonium ($P_{222(2O2O2)}^+$) cations. Agreement between simulations and experiments is good and permits a clear interpretation of the important topological differences between these systems. The first sharp diffraction peak (or prepeak) in the structure function $S(q)$ that is present in the case of the liquids containing the alkyl-substituted cations is absent in the case of the diether substituted analogs. Using different theoretical partitioning schemes for the X-ray structure function, we show that the prepeak present in the alkyl-substituted ILs arises from polarity alternations between charged groups and nonpolar alkyl tails. In the case of the diether substituted ILs, we find considerable curling of tails. Anions can be found with high probability in two different environments: close to the cationic nitrogen (phosphorus) and also close to the two ether groups. For the two diether systems, anions are found in locations from which they are excluded in the alkyl-substituted systems. This removes the longer range (polar/nonpolar) pattern of alternation that gives rise to the prepeak in alkyl-substituted systems.

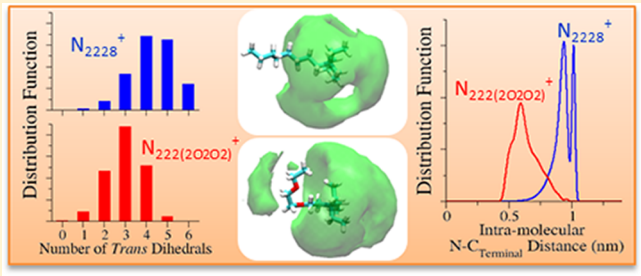

INTRODUCTION

During the past two decades, the unique properties of ionic liquids (ILs) have inspired research for a wide range of industrial and academic purposes.[1−6] ILs possess unique and peculiar properties not generally shared by conventional molecular liquids. In particular, research in the past several years has focused on understanding their morphology on the nanoscale. X-ray[7−29] and neutron scattering[30−32] experiments and molecular dynamics simulations[20,25,28,33−45] have been primary techniques to elucidate the microscopic structural ordering in these systems. Most cases studied to date involve cations with nonpolar alkyl chain substituents of different lengths. Only a few research reports can be found where nonpolar cationic tails are replaced in favor of other more polar substituents.[26,44,46−51]

ILs with tails modified by addition of polar components are often less viscous and more conducting,[52−56] two very desirable properties when facile transport is important.[52−58] The microscopic structure of these liquids is not yet fully understood and our goal is to derive a clear picture of what is expected when nonpolar tails are subject to discrete atomic changes that alter their polarity and spatial conformation. This article will show that the replacement of nonpolar alkyl chains by polar diether chains significantly changes the nanoscale organizational landscape of the ions.

METHODS

The four ionic liquids containing the cations $N_{222(2O2O2)}^+$, $P_{222(2O2O2)}^+$, N_{2228}^+, and P_{2228}^+ were prepared and purified as described previously.[52] To ensure low water content the ionic liquids were dried for 24 h on a Schlenk vacuum system, and the samples were prepared and sealed under an argon atmosphere in a glovebox.

X-ray Scattering Experiments. To obtain the structure functions for the four ionic liquids, X-ray scattering experiments

Received: November 7, 2012
Revised: December 19, 2012
Published: December 21, 2012

dx.doi.org/10.1021/jp311032p | J. Phys. Chem. B 2013, 117, 1130−1135

were carried out at the Advanced Photon Source, beamline 11-ID-C for values of the momentum transfer q in the range from 0.2 to 17 Å^{-1}. The protocols for sample preparation and X-ray experiments were previously published.[20,21,25] Raw data from the Perkin-Elmer amorphous silicon model 1621 AN3 CCD detector were processed using the Fit2D software from Hammersley et al.[59,60]

The raw scattering intensity data for liquids where NTf_2^- is paired with the $N_{222(2O2O2)}^+$, $P_{222(2O2O2)}^+$, N_{2228}^+, and P_{2228}^+ cations has been discussed previously.[49] Here we present the analysis of the full liquid structure functions. As we have done previously, the total scattering function $S(q)$ was calculated from the observed total scattering intensity $I_{coh}(q)$ using the PDFgetX2 program from Qui et al.[61]

Computational Details. All of the simulations were carried out using the GROMACS package[62,63] for 1000 ion pairs. We used the OPLS-AA[64−67] and Lopes and Pádua[68,69] parameters except in cases when these were unavailable. The full list of force field parameters as well as simulation and system equilibration details are available in the Supporting Information. The leapfrog algorithm was used for integration of the equations of motion at 292 K and 1 bar in the NPT ensemble. After thorough equilibration, all trajectories were subsequently run for 6 ns, and the last 2 ns of the equilibrated trajectory was used for the calculation of liquid properties. The calculation procedure for total structure functions and its ionic and subionic components have been well documented by our groups previously.[20,25,43,70,71]

RESULTS AND DISCUSSION

Figure 1 shows a comparison between experimental X-ray scattering structure functions $S(q)$ for alkyl-substituted ammonium

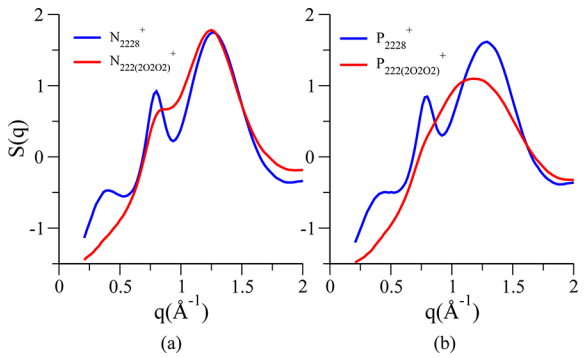

Figure 1. Experimental X-ray scattering structure functions $S(q)$ in the intermolecular region for (a) N_{2228}^+/NTf_2^- and $N_{222(2O2O2)}^+/NTf_2^-$ and (b) P_{2228}^+/NTf_2^- and $P_{222(2O2O2)}^+/NTf_2^-$ at 292 K.[49]

and phosphonium liquids versus the corresponding diether analogs. Three peaks are present in the intermolecular part of $S(q)$ for both of the alkyl-substituted ILs for values of q less than 2 Å^{-1}. These peaks are located at about 0.4, 0.8, and 1.3 Å^{-1}; by using the Bragg condition estimate of $2\pi/q_{peak}$, these correspond to characteristic real space distances of about 16, 8, and 5 Å, respectively. These three peaks are commonly observed in many ILs containing the NTf_2^- anion when cationic alkyl tails are moderately long.[14,17,19,25,49,70,72] The origin of these peaks has been previously explored.[17,22,25,43,70,71] In particular, we have demonstrated that the peak at 1.3 Å^{-1} is because of adjacency correlations associated with nearest neighbor as well as intramolecular interactions. The intermediate peak at 0.8 Å^{-1} is due to positive/negative ionic charge alternation, and the peak at lowest q value, the so-called prepeak or first sharp diffraction peak at 0.4 Å^{-1}, is often due to polar/nonpolar alternation. Interestingly, the prepeak that is present at 0.4 Å^{-1} in the cases of the N_{2228}^+ and P_{2228}^+ based ILs is absent in the cases of the $N_{222(2O2O2)}^+$ and $P_{222(2O2O2)}^+$ based ILs. Furthermore, different features in the diether containing liquids are broad and what appears as a well-defined peak at about 0.8 Å^{-1} in the case of the nonether systems becomes a shoulder in the case of the diether containing ILs.

In the case of the diether based ILs, we claim that the absence of the prepeak stems from the loss of anionic contribution to the longer length scale polar/nonpolar ordering. Before we go into details that prove this using unique partitions of the structure function, we present a pictorial demonstration of this using density isosurfaces in Figure 2. Two things are clear from

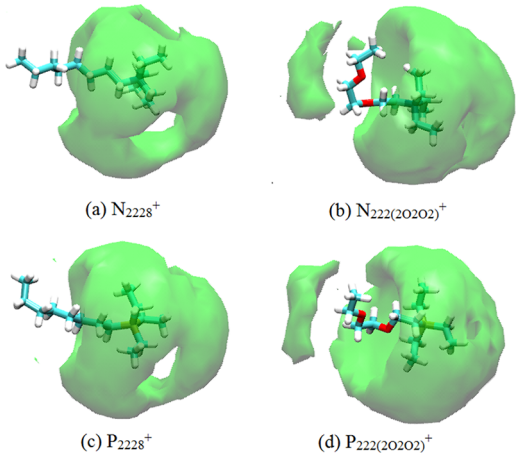

Figure 2. Isodensity spatial distribution functions for all atoms in the anions (green) surrounding (a) N_{2228}^+, (b) $N_{222(2O2O2)}^+$, (c) P_{2228}^+, and (d) $P_{222(2O2O2)}^+$ cations. To compute these isodensities, a representative cation was chosen, and all other cations were fitted to spatially overlap with it. All atom anionic densities were then computed around all the atoms in the cations. Note that anions are present only near the cation headgroup in the case of the alkyl-substituted ILs, but this is not the case for diether substituted systems where anions also cap the tails. In each case, isovalues were chosen to reflect the first solvation shell. Tail configurations have distinctly different geometries in both types of systems. It is common for tails to curl back toward the head in the case of the diether substituted systems.

Figure 2. First, the diether systems present tails that curl toward the cationic headgroup. See Figure 3 and Figures S2 and S3 in the Supporting Information for a quantitative description of this curling. Second, anions solvate both the cationic head and the tail in proximity to the ether groups. In other words, anions tend to cap both ends of the cation. This is in contrast to the ILs having nonpolar alkyl tails for which tails are less curled and for which there is depletion of anionic density close to the cationic tails but enhancement around cationic head groups. This depletion and enhancement in density correlations is an important factor contributing to the polar/nonpolar prepeak in the nonether systems and is the reason for the absence of this peak in the diether containing systems. With this description in mind we proceed to provide a more mathematical demonstration based on structure function partitionings.

Figure 4 shows a comparison between simulated and experimental $S(q)$ for all ILs studied here. All features present in the experimental $S(q)$ are also present in the simulated results

dx.doi.org/10.1021/jp311032p | J. Phys. Chem. B 2013, 117, 1130−1135

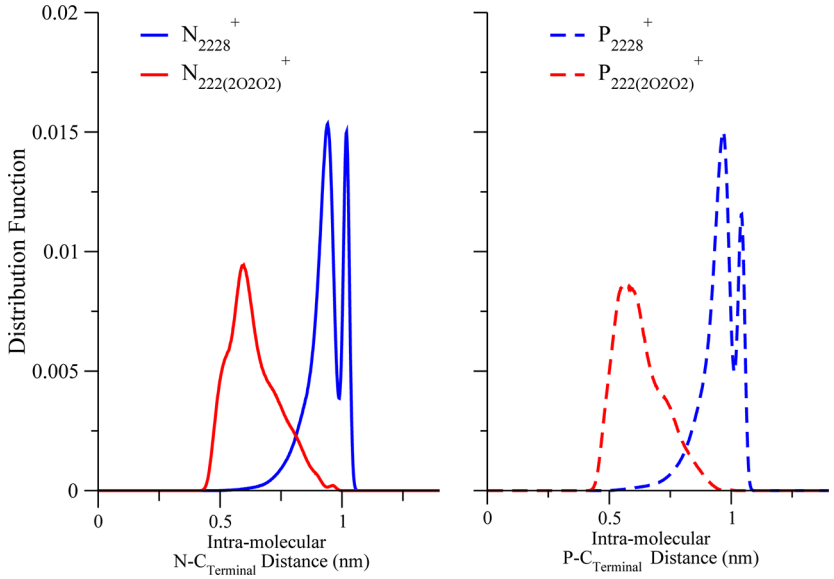

Figure 3. Intramolecular distance distribution function for distances between cationic nitrogen (phosphorus) and terminal carbon of longest tail for N_{2228}^+, $N_{222(2O2O2)}^+$ (left) and P_{2228}^+, $P_{222(2O2O2)}^+$ (right). The bimodal distribution in the case of the nonether system is very similar to that previously found in ref 73 and relates to the number of gauche kinks in the tail. The peak at larger distance in the octyl-cation liquids corresponds to mostly trans or a single gauche kink conformation, whereas the peak at lower distance corresponds to conformations with more kinks. In the case of the diether-cation liquids we observe a much broader distribution centered at much lower distances consistent with the curling of the tail.

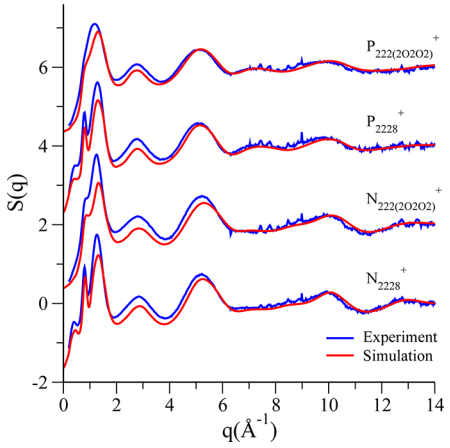

Figure 4. Comparison of simulated (red) vs experimental (blue) $S(q)$ for the N_{2228}^+/NTf_2^-, $N_{222(2O2O2)}^+/NTf_2^-$, P_{2228}^+/NTf_2^-, and $P_{222(2O2O2)}^+/NTf_2^-$ ILs at 292 K. Vertical offsets of +2, +4, and +6 have been applied for clarity. The spikes for q larger than 6 $Å^{-1}$ result from small systematic errors in the detector correction procedure.

at the same q values, but simulated peak heights appear to be somewhat lower. Since agreement is good overall, we use the simulated results to analyze in detail the structure of these systems.

First we analyze the structure function $S(q)$ for the ILs with alkyl substituted cations, N_{2228}^+ and P_{2228}^+. By partitioning the total $S(q)$ into its unique cation−cation, anion−anion, and cation−anion subcomponents in Figures 5a and c, we find that the anion−anion correlations are the most significantly positive going contributions to the prepeak at 0.4 $Å^{-1}$. This observation is consistent with several previous studies.[25,32,43,70] Other partitioning schemes for $S(q)$ (vide infra) demonstrate that cations also contribute to the prepeak, but these contributions are both negative going and positive going resulting in the overall cancellation. Kashyap and co-workers have previously explained this phenomenon in detail.[70,71]

Additional insight is gained by further partitioning the cationic contributions to $S(q)$ into head and tail parts, $S^{c-c}(q) = S^{c_{head}-c_{head}}(q) + S^{c_{head}-c_{tail}}(q) + S^{c_{tail}-c_{head}}(q) + S^{c_{tail}-c_{tail}}(q)$, as shown in Figures 6a and c. By resolving the distinct contributions from the polar head and nonpolar tail components of the cations, one can clearly appreciate that head−head and tail−tail correlations provide positive going contributions (peaks) to the prepeak, whereas cation head−tail correlations provide a negative going contribution (antipeak). The same pattern can be observed in Figures 7a and c where (cation head)−anion provides a peak and (cation tail)−anion provides an antipeak in the prepeak region around 0.4 $Å^{-1}$. We have explained in a recent set of articles[70,71] that this is the signature of polar/nonpolar alternation (as opposed to positive negative charge alternation, which occurs on a shorter length scale). Notice that peaks and antipeaks in the ionic subcomponents of $S(q)$ are not only present at the prepeak region but also appear in Figure 5 at 0.8 $Å^{-1}$. This is the shorter characteristic length scale corresponding to positive/negative charge alternation.

A clear prepeak is visible in the total $S(q)$ function as well as in the anion−anion subcomponent for the ILs with octyl substituted cations N_{2228}^+ and P_{2228}^+, as shown in Figures 5a and c, but the corresponding graphs for the ILs with diether substituted cations $N_{222(2O2O2)}^+$ and $P_{222(2O2O2)}^+$ show no sign of a prepeak (Figures 5b and d). Figures 6b and d show that, as opposed to the case of the alkyl substituted systems, the diether liquids show a much diminished head−head contribution to the prepeak, but tail−tail and head−tail components of $S(q)$ still show destructive interference between peaks and antipeaks. A similar phenomenon is observed in Figure 7. Whereas alkyl substituted systems display pronounced cationic head−anion prepeaks and cationic tail−anion antiprepeaks (Figures 7a and c), these features are much diminished in the case of the diether substituted systems (Figures 7b and d). This indicates a non-negligible but much weaker set of spatial correlations and anticorrelations between anions and cationic head or tail groups at this particular reciprocal distance.

dx.doi.org/10.1021/jp311032p | J. Phys. Chem. B 2013, 117, 1130−1135

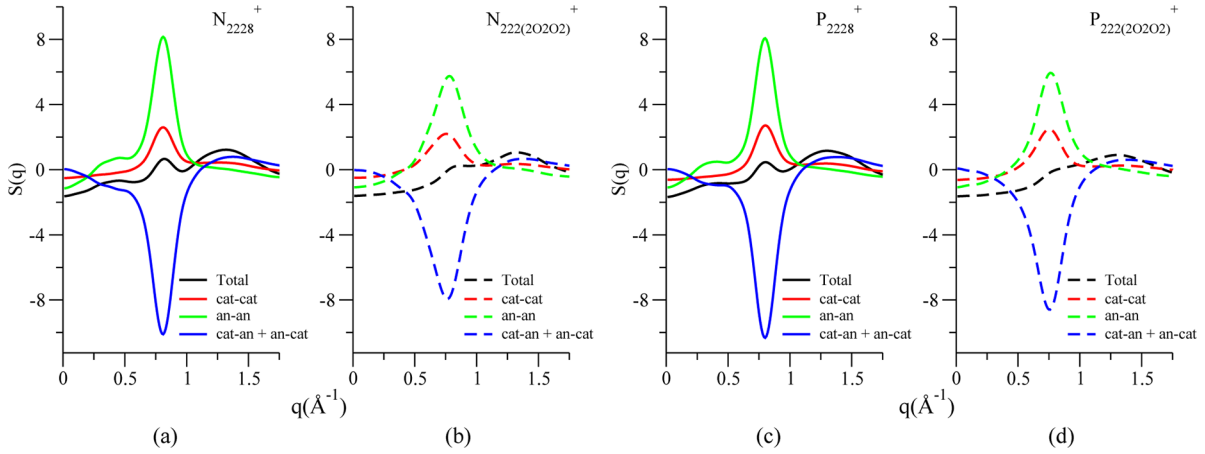

Figure 5. Total structure function $S(q)$ (black) resolved into cation−cation (red), anion−anion (green), and cation−anion (blue) partial components for (a) N_{2228}^{+}/NTf_2^{-}, (b) $N_{222(2O2O2)}^{+}/NTf_2^{-}$, (c) P_{2228}^{+}/NTf_2^{-}, and (d) $P_{222(2O2O2)}^{+}/NTf_2^{-}$.

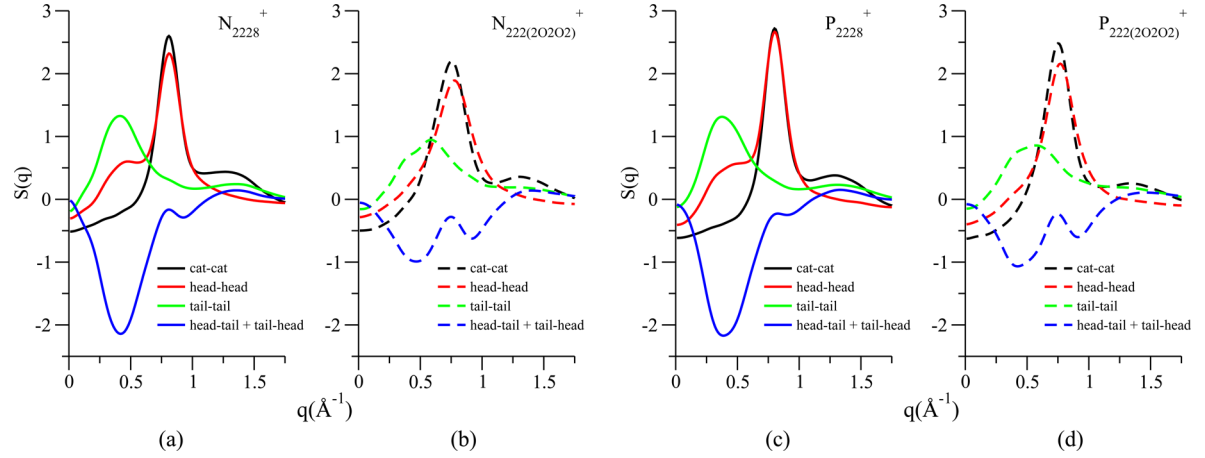

Figure 6. Cation−cation partial $S(q)$ (black) decomposed into head−head (red), tail−tail (green), and head−tail (blue) subcomponents for (a) N_{2228}^{+}/NTf_2^{-}, (b) $N_{222(2O2O2)}^{+}/NTf_2^{-}$, (c) P_{2228}^{+}/NTf_2^{-}, and (d) $P_{222(2O2O2)}^{+}/NTf_2^{-}$.

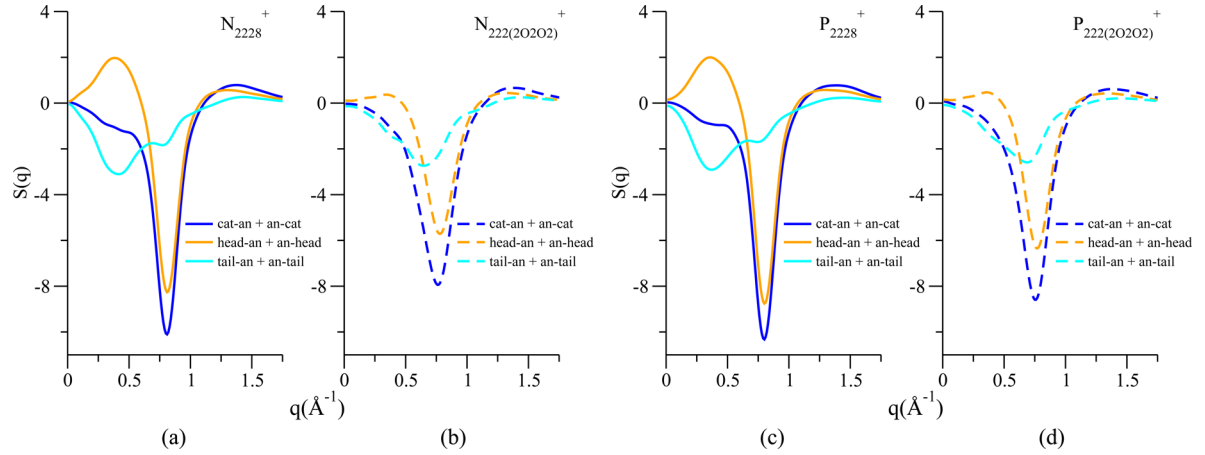

Figure 7. Cation−anion $S(q)$ (blue) split into cation head−anion (orange) and cation tail−anion (cyan) terms for (a) N_{2228}^{+}/NTf_2^{-}, (b) $N_{222(2O2O2)}^{+}/NTf_2^{-}$, (c) P_{2228}^{+}/NTf_2^{-}, and (d) $P_{222(2O2O2)}^{+}/NTf_2^{-}$.

CONCLUSIONS

When a prepeak is observed in X-ray experiments of ILs, this usually reflects the length scale of polar/nonpolar alternation. The replacement of the cationic nonpolar alkyl tails by the isoelectronic but polar diether groups significantly alters the organization of ionic liquids because the anions solvate not just the cationic head groups but also the polar tails. In conjunction with the curling of cationic tails, to a large extent this removes the typical polar−nonpolar ordering common in other ionic liquids with alkyl tails. This removal can be detected in real space by analyzing the arrangement of anions around cations in 3D spatial distribution functions. It can also be derived from ionic

dx.doi.org/10.1021/jp311032p | J. Phys. Chem. B 2013, 117, 1130−1135

and subionic partitionings of $S(q)$. These partitionings demonstrate that purely anionic contributions to the prepeak, which are most important in the case of alkyl substituted systems, are absent in the case of the diether substituted systems. The signatures of alternations due to cationic head−anion density enhancements and cationic tail−anion density depletions are also much diminished in the case of the diether systems.

■ ASSOCIATED CONTENT

Supporting Information

Computational details, supporting figures, and data. This material is available free of charge via the Internet at http://pubs.acs.org.

■ AUTHOR INFORMATION

Corresponding Author

*E-mail: ed.castner@rutgers.edu; claudio-margulis@uiowa.edu.

Notes

The authors declare no competing financial interest.

■ ACKNOWLEDGMENTS

This research was funded by the National Science Foundation under Grants CHE-1112033 (University of Iowa) and CHE-1112077 (Rutgers). The work by H.S. in Chiba was supported by the Ministry of Education, Culture, Sports, Science and Technology (MEXT) of Japan (Grant-in-Aid for Young Scientists (A): 21685001).

■ REFERENCES

(1) MacFarlane, D. R.; Huang, J.; Forsyth, M. *Nature* **1999**, *402*, 792−794.
(2) Wang, P.; Wenger, B.; Humphry-Baker, R.; Moser, J.-E.; Teuscher, J.; Kantlehner, W.; Mezger, J.; Stoyanov, E. V.; Zakeeruddin, S. M.; Gratzel, M. *J. Am. Chem. Soc.* **2005**, *127*, 6850−6856.
(3) Kuang, D.; Wang, P.; Ito, S.; Zakeeruddin, S. M.; Gratzel, M. *J. Am. Chem. Soc.* **2006**, *128*, 7732−7733.
(4) Han, X.; Armstrong, D. W. *Acc. Chem. Res.* **2007**, *40*, 1079−1086.
(5) Wishart, J. F. *Energy Environ. Sci.* **2009**, *2*, 956−961.
(6) Castner, E. W., Jr.; Wishart, J. F. *J. Chem. Phys.* **2010**, *132*, 120901.
(7) Bradley, A. E.; Hardacre, C.; Holbrey, J. D.; Johnston, S.; McMath, S. E. J.; Nieuwenhuyzen, M. *Chem. Mater.* **2002**, *14*, 629−635.
(8) Triolo, A.; Mandanici, A.; Russina, O.; Rodriguez-Mora, V.; Cutroni, M.; Hardacre, C.; Nieuwenhuyzen, M.; Bleif, H.-J.; Keller, L.; Ramos, M. A. *J. Phys. Chem. B* **2006**, *110*, 21357−21364.
(9) Triolo, A.; Russina, O.; Bleif, H.-J.; DiCola, E. *J. Phys. Chem. B* **2007**, *111*, 4641−4644.
(10) Triolo, A.; Russina, O.; Fazio, B.; Triolo, R.; DiCola, E. *Chem. Phys. Lett.* **2008**, *457*, 362−365.
(11) Atkin, R.; Warr, G. G. *J. Phys. Chem. B* **2008**, *112*, 4164−4166.
(12) Fukuda, S.; Takeuchi, M.; Fujii, K.; Kanzaki, R.; Takamuku, T.; Chiba, K.; Yamamoto, H.; Umebayashi, Y.; Ishiguro, S.-i. *J. Mol. Liq.* **2008**, *143*, 2−7.
(13) Fujii, K.; Seki, S.; Fukuda, S.; Takamuku, T.; Kohara, S.; Kameda, Y.; Umebayashi, Y.; Ishiguro, S.-i. *J. Mol. Liq.* **2008**, *143*, 64−69.
(14) Xiao, D.; Hines, L. G., Jr.; Li, S.; Bartsch, R. A.; Quitevis, E. L.; Russina, O.; Triolo, A. *J. Phys. Chem. B* **2009**, *113*, 6426−6433.
(15) Triolo, A.; Russina, O.; Fazio, B.; Appetecchi, G. B.; Carewska, M.; Passerini, S. *J. Chem. Phys.* **2009**, *130*, 164521.
(16) Russina, O.; Triolo, A.; Gontrani, L.; Caminiti, R.; Xiao, D.; Hines, L. G., Jr.; Bartsch, R. A.; Quitevis, E. L.; Pleckhova, N.; Seddon, K. R. *J. Phys.: Condens. Matter* **2009**, *21*, 424121.
(17) Gontrani, L.; Russina, O.; Celso, F. L.; Caminiti, R.; Annat, G.; Triolo, A. *J. Phys. Chem. B* **2009**, *113*, 9235−9240.
(18) Pott, T.; Méléard, P. *Phys. Chem. Chem. Phys.* **2009**, *11*, 5469−5475.
(19) Zheng, W.; Mohammed, A.; Hines, L. G.; Xiao, D.; Martinez, O. J.; Bartsch, R. A.; Simon, S. L.; Russina, O.; Triolo, A.; Quitevis, E. L. *J. Phys. Chem. B* **2011**, *115*, 6572−6584.
(20) Santos, C. S.; Annapureddy, H. V. R.; Murthy, N. S.; Kashyap, H. K.; Castner, E. W., Jr.; Margulis, C. J. *J. Chem. Phys.* **2011**, *134*, 064501.
(21) Santos, C. S.; Murthy, N. S.; Baker, G. A.; Castner, E. W., Jr. *J. Chem. Phys.* **2011**, *134*, 121101.
(22) Fujii, K.; Kanzaki, R.; Takamuku, T.; Kameda, Y.; Kohara, S.; Kanakubo, M.; Shibayama, M.; Ishiguro, S.-i.; Umebayashi, Y. *J. Chem. Phys.* **2011**, *135*, 244502.
(23) Hayes, R.; Imberti, S.; Warr, G. G.; Atkin, R. *Phys. Chem. Chem. Phys.* **2011**, *13*, 13544−13551.
(24) Umebayashi, Y.; Hamano, H.; Seki, S.; Minofar, B.; Fujii, K.; Hayamizu, K.; Tsuzuki, S.; Kameda, Y.; Kohara, S.; Watanabe, M. *J. Phys. Chem. B* **2011**, *115*, 12179−12191.
(25) Kashyap, H. K.; Santos, C. S.; Annapureddy, H. V. R.; Murthy, N. S.; Margulis, C. J.; Castner, E. W., Jr. *Faraday Discuss.* **2012**, *154*, 133−143.
(26) Russina, O.; Triolo, A. *Faraday Discuss.* **2012**, *154*, 97−109.
(27) Russina, O.; Triolo, A.; Gontrani, L.; Caminiti, R. *J. Phys. Chem. Lett.* **2012**, *3*, 27−33.
(28) Li, S.; Banuelos, J. L.; Guo, J.; Anovitz, L.; Rother, G.; Shaw, R. W.; Hillesheim, P. C.; Dai, S.; Baker, G. A.; Cummings, P. T. *J. Phys. Chem. Lett.* **2012**, *3*, 125−130.
(29) Castner, E. W., Jr.; Margulis, C. J.; Maroncelli, M.; Wishart, J. F. *Annu. Rev. Phys. Chem.* **2011**, *62*, 85−105.
(30) Triolo, A.; Russina, O.; Arrighi, V.; Juranyi, F.; Janssen, S.; Gordon, C. *J. Chem. Phys.* **2003**, *119*, 8549−8557.
(31) Hardacre, C.; Holbrey, J. D.; Nieuwenhuyzen, M.; Youngs, T. G. A. *Acc. Chem. Res.* **2007**, *40*, 1146−1155.
(32) Hardacre, C.; Holbrey, J. D.; Mullan, C. L.; Youngs, T. G. A.; Bowron, D. T. *J. Chem. Phys.* **2010**, *133*, 74510−74517.
(33) Urahata, S. M.; Ribeiro, M. C. *J. Chem. Phys.* **2004**, *120*, 1855−1863.
(34) Del Popolo, M. G.; Voth, G. A. *J. Phys. Chem. B* **2004**, *108*, 1744−1752.
(35) Wang, Y.; Voth, G. A. *J. Am. Chem. Soc.* **2005**, *127*, 12192−12193.
(36) Wang, Y.; Voth, G. A. *J. Phys. Chem. B* **2006**, *110*, 18601−18608.
(37) Borodin, O.; Smith, G. D. *J. Phys. Chem. B* **2006**, *110*, 11481−11490.
(38) Deetlefs, M.; Hardacre, C.; Nieuwenhuyzen, M.; Pádua, A. A. H.; Sheppard, O.; Soper, A. K. *J. Phys. Chem. B* **2006**, *110*, 12055−12061.
(39) Bhargava, B. L.; Devane, R.; Klein, M. L.; Balasubramanian, S. *Soft Matter* **2007**, *3*, 1395−1400.
(40) Lopes, J. N. C.; Pádua, A. A. H. *J. Phys. Chem. B* **2006**, *110*, 3330−3335.
(41) Canongia Lopes, J. N.; Shimizu, K.; Pádua, A. A. H.; Umebayashi, Y.; Fukuda, S.; Fujii, K.; Ishiguro, S.-i. *J. Phys. Chem. B* **2008**, *112*, 1465−1472.
(42) Liu, X.; Zhou, G.; Zhang, S.; Yu, G. *Mol. Simul.* **2010**, *36*, 79−86.
(43) Annapureddy, H. V. R.; Kashyap, H. K.; De Biase, P. M.; Margulis, C. J. *J. Phys. Chem. B* **2010**, *114*, 16838−16846.
(44) Siqueira, L. J. A.; Ribeiro, M. C. C. *J. Chem. Phys.* **2011**, *135*, 204506.
(45) Liu, X.; Zhao, Y.; Zhang, X.; Zhou, G.; Zhang, S. *J. Phys. Chem. B* **2012**, *116*, 4934−4942.
(46) Siqueira, L. J. A.; Ribeiro, M. C. C. *J. Phys. Chem. B* **2007**, *111*, 11776−11785.
(47) Smith, G. D.; Borodin, O.; Li, L.; Kim, H.; Liu, Q.; Bara, J. E.; Gin, D. L.; Nobel, R. *Phys. Chem. Chem. Phys.* **2008**, *10*, 6301−6312.

(48) Siqueira, L. J. A.; Ribeiro, M. C. C. *J. Phys. Chem. B* **2009**, *113*, 1074−1079.
(49) Triolo, A.; Russina, O.; Caminiti, R.; Shirota, H.; Lee, H. Y.; Santos, C. S.; Murthy, N. S.; Castner, E. W., Jr. *Chem. Commun.* **2012**, *48*, 4959−4961.
(50) Pensado, A. S.; Gomes, M. F. C.; Lopes, J. N. C.; Malfreyt, P.; Pádua, A. A. H. *Phys. Chem. Chem. Phys.* **2011**, *13*, 13518−13526.
(51) Pensado, A. S.; Pádua, A. A. H.; Costa Gomes, M. F. *J. Phys. Chem. B* **2011**, *115*, 3942−3948.
(52) Shirota, H.; Fukazawa, H.; Fujisawa, T.; Wishart, J. F. *J. Phys. Chem. B* **2010**, *114*, 9400−9412.
(53) Yamaguchi, T.; Mikawa, K.; Koda, S.; Fukazawa, H.; Shirota, H. *Chem. Phys. Lett.* **2012**, *521*, 69−73.
(54) Deng, Y.; Husson, P.; Delort, A.-M.; Besse-Hoggan, P.; Sancelme, M.; Costa Gomes, M. F. *J. Chem. Eng. Data* **2011**, *56*, 4194−4202.
(55) Tang, S.; Baker, G. A.; Zhao, H. *Chem. Soc. Rev.* **2012**, *41*, 4030−4066.
(56) Ueno, K.; Yoshida, K.; Tsuchiya, M.; Tachikawa, N.; Dokko, K.; Watanabe, M. *J. Phys. Chem. B* **2012**, *116*, 11323−11331.
(57) Howlett, P. C.; Izgorodina, E. I.; Forsyth, M.; MacFarlane, D. R. *Z. Phys. Chem.* **2006**, *220*, 1483−1498.
(58) Henderson, W. A.; Young, V. G.; Pearson, W.; Passerini, S.; De Long, H. C.; Trulove, P. C. *J. Phys.: Condens. Matter* **2006**, *18*, 10377−10390.
(59) Hammersley, A.; Svensson, S.; Hanfland, M.; Fitch, A.; Hausermann, D. *High Pressure Res.* **1996**, *14*, 235−248.
(60) Hammersley, A. P. *FIT2D V10.3 Reference Manual V4.0*; European Synchrotron Radiation Facility: Grenoble, France, 1998.
(61) Qui, X.; Thompson, J. W.; Billinge, S. J. L. *J. Appl. Crystallogr.* **2004**, *37*, 678.
(62) Hess, B.; Kutzner, C.; van der Spoel, D.; Lindahl, E. *J. Chem. Theory Comput.* **2008**, *4*, 435−447.
(63) van der Spoel, D.; Lindahl, E.; Hess, B.; Groenhof, G.; Mark, A. E.; Berendsen, H. J. C. *J. Comput. Chem.* **2005**, *26*, 1701−1718.
(64) Jorgensen, W. L.; Maxwell, D. S.; Tirado-Rives, J. *J. Am. Chem. Soc.* **1996**, *118*, 11225−11236.
(65) Kaminski, G.; Jorgensen, W. L. *J. Phys. Chem.* **1996**, *100*, 18010−18013.
(66) Rizzo, R. C.; Jorgensen, W. L. *J. Am. Chem. Soc.* **1999**, *121*, 4827−4836.
(67) Price, M. L. P.; Ostrovsky, D.; Jorgensen, W. L. *J. Comput. Chem.* **2001**, *22*, 1340−1352.
(68) Lopes, J. N. C.; Pádua, A. A. H. *J. Phys. Chem. B* **2004**, *108*, 16893−16898.
(69) Canongia Lopes, J. N.; Pádua, A. A. H. *J. Phys. Chem. B* **2006**, *110*, 19586−19592, PMID: 17004824.
(70) Kashyap, H. K.; Hettige, J. J.; Annapureddy, H. V. R.; Margulis, C. J. *Chem. Commun.* **2012**, *48*, 5103−5105.
(71) Kashyap, H. K.; Margulis, C. J. *ECS Trans.* **2012**, *50*, 301−307.
(72) Bodo, E.; Gontrani, L.; Caminiti, R.; Plechkova, N. V.; Seddon, K. R.; Triolo, A. *J. Phys. Chem. B* **2010**, *114*, 16398−16407.
(73) Margulis, C. *Mol. Phys.* **2004**, *102*, 829−838.